

Divergent stiffness of one-dimensional growing interfaces

Mutsumi Minoguchi and Shin-ichi Sasa

Department of Physics, Kyoto University, Kyoto 606-8502, Japan

(Dated: October 9, 2024)

When a spatially localized stress is applied to a growing one-dimensional interface, the interface deforms. This deformation is described by the effective surface tension representing the stiffness of the interface. We present that the stiffness exhibits divergent behavior in the large system size limit for a growing interface with thermal noise, which has never been observed for equilibrium interfaces. Furthermore, by connecting the effective surface tension with a space-time correlation function, we elucidate the mechanism that anomalous dynamical fluctuations lead to divergent stiffness.

Introduction.— The statistical behavior of many-interacting elements out of equilibrium has attracted attention for a wide range of systems [1–3]. A remarkable feature of such systems is that the standard relations in equilibrium systems no longer hold. For example, phase order is not observed in two dimensions at finite temperatures for equilibrium systems [4, 5], while phase order emerges in two dimensions for active matters [6] or sheared systems [7]. The particular nature of out-of-equilibrium systems is not limited to phase transition problems. As the simplest example, let us consider the response against a perturbation. When an inhomogeneous stress is imposed on an equilibrium system, the response remains finite except for particular states such as a phase transition point, because the perturbation is calculated using the canonical distribution. In contrast, the response in systems out of equilibrium may give rise to a singular behavior without tuning system conditions. In this Letter, we study such a generic singular response out of equilibrium.

Specifically, a one-dimensional interface, whose height is defined in $0 \leq x \leq L$, is investigated. The interface deforms when a localized stress is applied. For equilibrium interfaces [8], their shape in the linear response regime is expressed by a quadratic function of x , where its curvature is determined by the surface tension κ . This is understood by considering a simple model within equilibrium statistical mechanics. Now, let us consider growing interfaces [10]. The deformation against the weak localized stress is still described by a quadratic function of x , and the curvature of the interface is characterized by the effective surface tension κ_{eff} . Then, it can be found that κ_{eff} is greater than κ , as shown in Fig 1. Moreover, as the singular behavior in this case, κ_{eff} for a larger system size L is found to be large, as shown in Fig. 2. In other words, growing interfaces exhibit singular stiffness.

From a theoretical viewpoint, an important aspect related to the singular response is that the stationary distribution under a perturbation can be formally expressed in terms of the time integration of the perturbation effect [11–13]. In other words, a local perturbation typically leads to a wide range of influences through time evolution, except for special cases where such time integration is evaluated from a detailed balance condition, as in equilibrium systems. An illustrative example

of this phenomenon is the blowtorch effect where the relative distribution of some configurations can be controlled by modifying the kinetics far from the configurations [14]. Therefore, it is possible that the stationary distribution is singularly perturbed by the local stress.

To make sure the singularity, a formula describing the response should be established. This problem is reminiscent of the standard linear response theory around an equilibrium state. For example, when considering heat conduction for a Hamiltonian system in contact with two heat baths with temperatures T_1 and T_2 , $T_2 - T_1$ is treated as a perturbation [15]. In this case, the linear response formula is the Green-Kubo formula, which expresses the conductivity in terms of the time integration of the current correlation function at equilibrium [11]. Similarly to heat conduction, we expect that the effective surface tension κ_{eff} can be expressed as the time integration of a certain time correlation function. In this Letter, we derive such a formula using a generalized fluctuation theorem associated with the excess entropy production.

Based on the response formula, the singular stiffness is investigated. As is known, some low-dimensional systems exhibit an anomaly in the large-distance and long-time properties of the time correlation function [15]. In such systems, the decay rate of a time correlation function is so small that its time integration is not bounded in the large system size limit [15–17]. By combining this property with the response formula, the divergent behavior of the stiffness out of equilibrium can be explicitly determined.

Setup.— The one-dimensional interface defined in $0 \leq x \leq L$ is investigated. The height of the interface at time t is expressed by $h(x, t)$, which is collectively denoted by $\hat{h} = (h(x))_{x=0}^L$. For simplicity, the periodic boundary condition $h(0, t) = h(L, t)$ is assumed. An external stress $\epsilon p_{\text{ex}}(x)$ is imposed on the interface, where the total force $\epsilon \int p_{\text{ex}}(x) dx$ is set to zero to avoid the additional drift of the interface. The free energy of the interface is assumed to be

$$F^\epsilon(\hat{h}) \equiv \int_0^L dx \left[\frac{\kappa}{2} (\partial_x h)^2 - \epsilon p_{\text{ex}}(x) h(x) \right], \quad (1)$$

where κ represents the surface tension. For equilibrium cases, the fluctuation properties are described by the

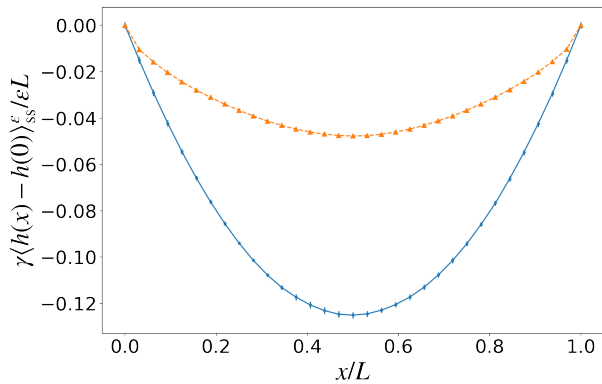


FIG. 1. Time-averaged patterns in steady state under the external stress with $\epsilon/\gamma = 0.01$. The system size is $L = 16$. The curvature of the growing interface ($v_0 = 5$, upper side) is smaller than that of the equilibrium interface ($v_0 = 0$, lower side).

following stochastic model [8]:

$$\partial_t h = -\frac{1}{\gamma} \frac{\delta F(\hat{h})}{\delta h} + \sqrt{\frac{2T}{\gamma}} \xi, \quad (2)$$

where γ is the dissipation constant; T is the temperature of the bath with the Boltzmann constant set to unity; ξ is the Gaussian white noise satisfying

$$\langle \xi(x, t) \xi(x', t') \rangle = \delta(x - x') \delta(t - t'). \quad (3)$$

Thus, it is immediately confirmed that the expectation of the interface shape under the external stress is given by

$$\kappa \partial_x^2 \langle h(x) \rangle_{\text{eq}}^\epsilon + \epsilon p_{\text{ex}}(x) = 0, \quad (4)$$

where $\langle \cdot \rangle_{\text{eq}}^\epsilon$ denotes the expectation in the equilibrium state of the system with the external stress $\epsilon p_{\text{ex}}(x)$. For simplicity, focus is placed on the case where $p_{\text{ex}}(x) = \delta(x) - 1/L$. By solving (4) [9], we obtain

$$\langle (h(x) - h(0)) \rangle_{\text{eq}}^\epsilon = \frac{\epsilon}{2L\kappa} \left[\left(x - \frac{L}{2} \right)^2 - \frac{L^2}{4} \right]. \quad (5)$$

Now, let us consider a growing interface described by

$$\partial_t h = v_0 + \frac{v_0}{2} (\partial_x h)^2 - \frac{1}{\gamma} \frac{\delta F_\epsilon(\hat{h})}{\delta h} + \sqrt{\frac{2T}{\gamma}} \xi, \quad (6)$$

as a generalization of (2), where $v_0 \geq 0$ is the propagation velocity of the flat interface. When $\epsilon = 0$, (6) is equivalent to the Kardar-Parisi-Zhang (KPZ) equation [10], which reproduces the dynamics of growing interfaces, such as the surface of growing crystal, water soaking into paper, and growing bacterial colony. It has been attracting attention in various fields, because interfaces appear at almost all scales of interest in science [2, 18]. Consequently, the KPZ equation has been extensively

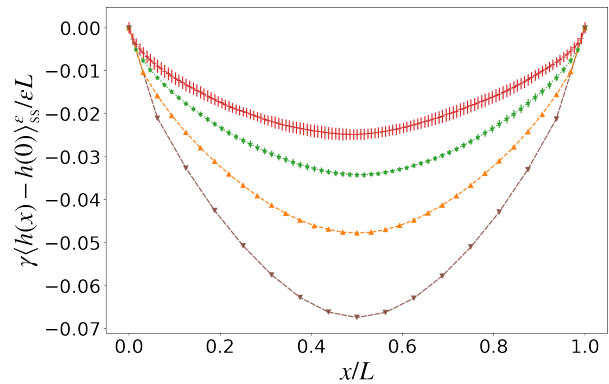


FIG. 2. System size dependence of the curve for $v_0 = 5$ in Fig.1. The patterns of $L = 8, 16, 32$, and 64 are shown from top to bottom. Although the equilibrium ($v_0 = 0$) interface does not depend on L , the growing interface becomes stiffer for larger L .

investigated through numerical [19–25], theoretical [26–32], and even mathematical [33–40] approaches. The system given by (6) is interpreted as a perturbed KPZ equation.

Numerical observation.— Let $\langle h(x) - h(0) \rangle_{\text{ss}}^\epsilon$ be the expectation of $h(x) - h(0)$ with respect to the steady state of (6). As an illustration, first, we numerically investigate $\langle h(x) - h(0) \rangle_{\text{ss}}^\epsilon$ for the specific parameter values $\kappa = T = \gamma = 1$ and $v_0 = 5$. Throughout this study, the numerical simulations were conducted using a spatially discretized model with a space interval $\Delta x = 0.5$ [9, 21]. The shapes of the growing interfaces shown in Fig. 2 are fitted to the following form:

$$\langle (h(x) - h(0)) \rangle_{\text{ss}}^\epsilon = \frac{\epsilon}{2L\kappa_{\text{eff}}} \left[\left(x - \frac{L}{2} \right)^2 - \frac{L^2}{4} \right], \quad (7)$$

which is the generalization of (5) with the replacement of κ by κ_{eff} , where ϵ is assumed to be sufficiently small. The fitting parameter κ_{eff} is interpreted as the effective surface tension characterizing the stiffness of the growing interface. Fig. 1 shows that κ_{eff} is greater than κ . In other words, the growing interface is stiffer than the equilibrium interface. Furthermore, as shown in Fig. 2, κ_{eff} increases for a larger system size L .

Now, two issues naturally arise. The first issue is quantifying the L dependence of κ_{eff} . From the viewpoint of numerical calculation, however, it becomes harder to accurately observe a slight shift of $\langle h(x) - h(0) \rangle_{\text{ss}}^\epsilon$ caused by the external stress for larger systems. The second issue is to investigate the mechanism of the L dependence. Both issues can be resolved by formulating a fluctuation-response relation for the system under investigation, where κ_{eff} is expressed by dynamical properties of fluctuations in a system without the external stress.

Response formula.— Let $[\hat{h}]$ be a trajectory $(\hat{h}(t))_{t=0}^\tau$. We consider any quantity $A([\hat{h}])$ satisfying $A([\hat{h} + \hat{c}]) = A([\hat{h}])$, where \hat{c} is a constant function in x . For such

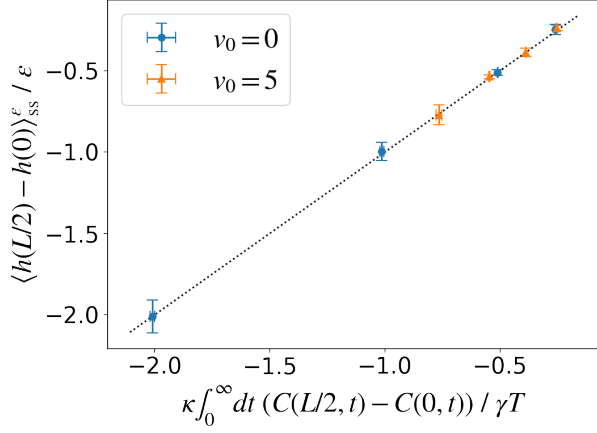


FIG. 3. Comparison of the left-hand side and the right-hand side of (13). The former is estimated by the direct calculation of the response for $\epsilon > 0$, while the latter is calculated in the system with $\epsilon = 0$. The round-blue and triangular-orange symbols represent the data for $v_0 = 0$ ($L = 2, 4, 8, 16$) and $v_0 = 5$ ($L = 2, 4, 8, 16$), respectively. These symbols should be on the dotted line if the left and right hand sides of (13) are equal.

$A([\hat{h}])$, we define A^* as $A^*([\hat{h}]) \equiv A([\hat{h}]^*)$ with $[\hat{h}]^* \equiv (\hat{h}(\tau - t))_{t=0}^\tau$, which represents the time-reversal of $[\hat{h}]$. For equilibrium cases $v_0 = 0$, the detailed balance condition $\langle A \rangle_{\text{eq}}^\epsilon = \langle A^* \rangle_{\text{eq}}^\epsilon$ holds for any ϵ , and the stationary distribution is given by

$$P_{\text{eq}}^\epsilon(h) = \frac{1}{Z} \exp(-\beta F^\epsilon(h)) \quad (8)$$

with $\beta = T^{-1}$. This also leads to (4).

However, for growing interfaces with $v_0 > 0$, the detailed balance condition does not hold. The extent of the violation is expressed by the entropy production

$$\sigma = \frac{\gamma}{T} \int_0^\tau dt \int_0^L dx (\partial_t h) \left(v_0 + \frac{v_0}{2} (\partial_x h)^2 \right), \quad (9)$$

which is the work done by the non-conservative force divided by the temperature. Using this thermodynamic entropy production, we arrive at the standard fluctuation theorem [41–44]

$$\langle A \rangle_{\text{tr}}^I = \langle A^* e^{-\sigma} \rangle_{\text{tr}}^I, \quad (10)$$

where $\langle \cdot \rangle_{\text{tr}}^I$ denotes the ensemble average over noise realizations and the initial conditions sampled from the stationary distribution with $v_0 = 0$.

Next, we notice another time-reversal transformation: $[\hat{h}]^\dagger \equiv (-\hat{h}(\tau - t))_{t=0}^\tau$. We then find $\langle A \rangle_{\text{ss}}^0 = \langle A^\dagger \rangle_{\text{ss}}^0$ for $A^\dagger([\hat{h}]^\dagger) \equiv A([\hat{h}])$ [9], which has been known since 1977 [16]. However, this time-reversal symmetry does not hold for interfaces under the external stress $\epsilon > 0$. This violation is expressed as

$$\langle A \rangle_{\text{tr}}^{II} = \langle A^\dagger e^{-\tilde{\sigma}} \rangle_{\text{tr}}^{II} \quad (11)$$

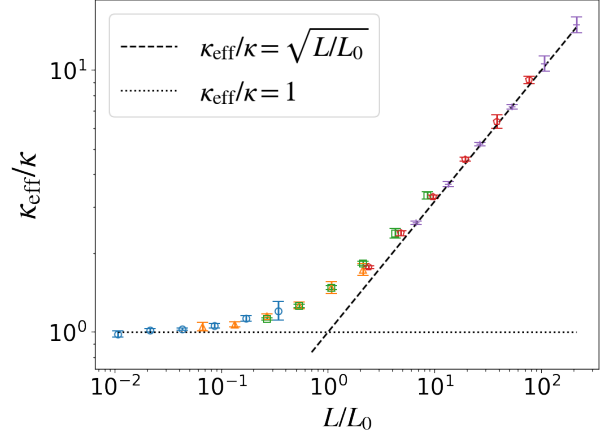


FIG. 4. System size dependence of κ_{eff} . The symbols are the numerical results for $L = 16, 32, 64, 128, 256$, and 512 for $v_0 = 0.2, 0.5, 1, 3$, and 5 . κ_{eff} maintains the same value as κ for $L \ll L_0$ and diverges as $(L/L_0)^{1/2}$ for $L \gg L_0$.

with

$$\tilde{\sigma} \equiv -\frac{\epsilon \kappa}{\gamma T} \int_0^\tau dt \int_0^L dx p_{\text{ex}}(x) \frac{\partial^2 h(x, t)}{\partial x^2}, \quad (12)$$

where $\langle \cdot \rangle_{\text{tr}}^{II}$ denotes the ensemble average over the noise realizations and initial conditions sampled from the stationary distribution without the external stress. We name (11) a generalized fluctuation theorem. Note that $\tilde{\sigma}$ is not the thermodynamic entropy production, but interpreted as the excess entropy production associated with the external stress [45].

Here, we set $A = h(x, \tau) - h(0, \tau)$, substitute it into (11), take the limit $\tau \rightarrow \infty$, and expand the right-hand side of (11) in ϵ . Noting that $\langle A \rangle_{\text{tr}}^{II}$ goes to $\langle h(x) - h(0) \rangle_{\text{ss}}^\epsilon$, we obtain [9]

$$\lim_{\epsilon \rightarrow 0} \frac{\langle h(x) - h(0) \rangle_{\text{ss}}^\epsilon}{\epsilon} = \frac{\kappa}{\gamma T} \int_0^\infty dt (C(x, t) - C(0, t)) \quad (13)$$

with

$$C(x, t) \equiv \langle \partial_x h(x, 0) \partial_x h(0, t) \rangle_{\text{ss}}^0. \quad (14)$$

This relation is interpreted as the fluctuation-response relation of the system under investigation. (13) is understood from the fluctuation-dissipation theorem for classical stochastic processes [46–48]. However, to our best knowledge, an explicit formula connecting the response to an external perturbation has never been proposed to date. We numerically check the validity of (13) for small systems with $L = 2, 4, 8$, and 16 . In Fig. 3, the left-hand side of (13) is plotted against the right-hand side of (13) at $x = L/2$ for both cases of $v_0 = 0$ and $v_0 = 5$. The result confirms that (13) holds.

Divergent stiffness.— As explained above, the numerical calculation of κ_{eff} defined by (7) is not easy to carry out for large systems. Thus, using the response formula

(13), we study the stiffness of the growing interface. Specifically, from (7) and (13), we obtain

$$\kappa_{\text{eff}} = -\frac{\gamma TL}{8\kappa} \left\{ \int_0^\infty dt \left[C\left(\frac{L}{2}, t\right) - C(0, t) \right] \right\}^{-1}. \quad (15)$$

By dimensional analysis, we find that $\kappa_{\text{eff}}/\kappa$ is expressed as a function of L/L_0 with

$$L_0 = \frac{\ell\kappa^3}{T\gamma^2v_0^2}, \quad (16)$$

where ℓ is a numerical constant corresponding to the dimensionless length characterizing the cross-over [9]. In other words, the following equation is obtained using a scaling function f whose form has not been determined yet:

$$\kappa_{\text{eff}} = \kappa f\left(\frac{L}{L_0}\right). \quad (17)$$

First, we notice that $\kappa_{\text{eff}} \rightarrow \kappa$ as $L_0 \rightarrow \infty$, because $v_0 \rightarrow 0$ refers to the equilibrium limit. To find the functional form of f , the right-hand side of (15) is numerically calculated for several values of L and v_0 for fixed $\kappa = T = \gamma = 1$. The numerical results with $\ell = 60$ are plotted in Fig. 4, such that the following equation holds for $L \gg L_0$:

$$\kappa_{\text{eff}} = \kappa \left(\frac{L}{L_0}\right)^{1/2}, \quad (18)$$

as indicated by the dotted line in Fig. 4. It is found that the data points for $L \geq 16$ are on one curve, which determines the form of the scaling function f . Note that those for $L \leq 8$ deviate from the curve [9]. This means that small-sized systems are not a good approximation of the KPZ equation. From Fig. 4, it is concluded that L_0 with $\ell \simeq 60$ provides the cross-over length from the normal response to the singular response, where the stiffness κ_{eff} shows the divergence as a function of L/L_0 , which is the main result of this Letter.

The divergent stiffness comes from a dynamical singularity of the correlation function $C(x, t)$, as suggested in the formula expressed by (15). The relation is explained in detail. Let $\tilde{C}(k, t)$ be the Fourier transform of $C(x, t)$. By dimensional analysis, we obtain

$$\int_0^\infty dt \tilde{C}(k, t) = \frac{\gamma T}{\kappa^2 k^2} \Phi\left(\frac{k\kappa^3}{T\gamma^2v_0^2}\right) \quad (19)$$

with a scaling function Φ . In the equilibrium limit $v_0 \rightarrow 0$, Φ should be equal to one, based on direct calculation. Now, let us consider the case $L \rightarrow \infty$ with fixed $v_0 \neq 0$. As is known, $\tilde{C}(k, t)$ has the scaling form $g(k^2t)$ in the limit $L \rightarrow \infty$, where the dynamical exponent z is given by $z = 3/2$ [10, 16]. By substituting this result into the left-hand side of (19), we find [9]

$$\Phi\left(\frac{k\kappa^3}{T\gamma^2v_0^2}\right) = c \left(\frac{|k|\kappa^3}{T\gamma^2v_0^2}\right)^{1/2}, \quad (20)$$

where the numerical constant c is calculated as $c = 2.43$ by the analysis of an exactly solvable stochastic model [30]. For finite but large L cases, it is assumed that (20) holds with the replacement of k by $k_n = 2\pi n/L$, where n is an integer satisfying $-n_c \leq n \leq n_c$. The cutoff integer n_c is given by $n_c = L/(2\Delta x)$. We then obtain [9]

$$\begin{aligned} & \int_0^\infty dt [C(L/2, t) - C(0, t)] \\ &= -\sqrt{L} \left(\frac{16c^2}{8\pi^3}\right)^{1/2} \left(\frac{T}{\kappa v_0^2}\right)^{1/2} \sum_{n=1}^{n_c/2} \frac{1}{(2n-1)^{3/2}}. \end{aligned} \quad (21)$$

By substituting (21) into (15), $\kappa_{\text{eff}} = \kappa(L/L_0^{\text{est}})^{1/2}$ holds with $L_0^{\text{est}} = \ell^{\text{est}}\kappa^3/(T\gamma^2v_0^2)$, where the numerical constant ℓ^{est} is calculated as

$$\ell^{\text{est}} = \frac{(32c)^2}{(2\pi)^3} \left(\sum_{n=1}^{n_c/2} \frac{1}{(2n-1)^{3/2}}\right)^2. \quad (22)$$

Therefore, the divergent stiffness arises from the singularity expressed by (20). The \sqrt{L} dependence of κ_{eff} corresponds to the $k^{3/2}$ dependence of $\int_0^\infty dt \tilde{C}(k, t)$. The cross-over length L_0 observed in the numerical simulations is predictable by considering the asymptotic form of $\int_0^\infty dt \tilde{C}(k, t)$. Indeed, the value $\ell \simeq 60$ obtained by the numerical simulations is consistent with (22). For example, $\ell^{\text{est}} = 62.5$ for $n_c = 128$. When investigating infinitely large systems, the limit $n_c \rightarrow \infty$ should be taken. In this case, ℓ^{est} approaches 69.52 [9].

Concluding remarks.— This Letter reports the singular response of a growing interface to the localized external stress. By defining the effective surface tension κ_{eff} by (7), the response formula (15) expressing κ_{eff} is formulated in terms of the time correlation function $C(x, t)$ of $\partial_x h(x, t)$. By numerically calculating the right-hand side of (15), it is found that $\kappa_{\text{eff}} = \kappa(L/L_0)^{1/2}$ for $L \gg L_0$ and $\kappa_{\text{eff}} = \kappa$ for $L \ll L_0$, where the cross-over length is given by (16). It is shown that the divergent stiffness comes from the dynamical singularity expressed by (20).

This study focused on the growing interface in the equilibrium environment, which is described by (6). However, the stochastic dynamics of the interface can be observed in a much wider context [49]. Keeping the universality in mind, we study the KPZ equation

$$\partial_t h = \frac{\lambda}{2} (\partial_x h)^2 + \nu \partial_x^2 h + \sqrt{2D} \xi \quad (23)$$

defined in $0 \leq x \leq L$. By adding the localized force term $\epsilon \delta(x)$ to the right-hand side of (23), ν_{eff} instead of κ_{eff} can be operationally defined through (7). Then, by using the result obtained above, it can be found that $\nu_{\text{eff}} = \nu(L/L_0)^{1/2}$ with $L_0 = \ell\nu^3/(D\lambda^2)$ for $L \gg L_0$, and $\nu_{\text{eff}} = \nu$ for $L \ll L_0$. The length L_0 characterizes the cross-over to the singular response from the normal response. The formula can be used to estimate the parameter values of the KPZ equation when there exists

a phenomenon that may be effectively described by the KPZ equation. Specifically, because ν_{eff} is a measurable quantity, one can estimate $\nu^3/(D\lambda^2)$ from the observational data of ν_{eff} for several values of L . From the fluctuation spectrum of $\partial_x h$, D/ν is determined. The parameter λ is determined from the average propagation velocity and the fluctuations. These three data lead

to ν , D , and λ . For example, it has been conjectured that the large distance and long-time behavior in the Kuramoto-Sivashinsky (KS) equation can be described by the KPZ equation [50–53]. Studying the KS equation from this viewpoint is an interesting topic of inquiry.

We thank K. Takeuchi for fruitful discussions. This study was supported by JSPS KAKENHI (Grant Numbers JP19H05795, JP20K20425, and JP22H01144).

-
- [1] F. Jülicher, S. W. Grill, and G. Salbreux, Hydrodynamic theory of active matter, *Rep. Prog. Phys.* **81**, 076601 (2018).
- [2] K. A. Takeuchi, An appetizer to modern developments on the Kardar-Parisi-Zhang universality class, *Physica A* **504**, 77-105 (2018).
- [3] J. Eisert, M. Friesdorf, and C. Gogolin, Quantum many-body systems out of equilibrium, *Nature Physics* **11**, 124-130 (2015).
- [4] P. C. Hohenberg, Existence of long-range order in one and two dimensions, *Phys. Rev.* **158**, 383-386 (1967).
- [5] N. D. Mermin and H. Wagner, Absence of ferromagnetism or antiferromagnetism in one- or two-dimensional isotropic Heisenberg models, *Phys. Rev. Lett.* **17**, 1133-1136 (1966).
- [6] J. Toner and Y. Tu, Long-range order in a two-dimensional dynamical XY model: How birds fly together, *Phys. Rev. Lett.* **75**, 4326-4329 (1995).
- [7] H. Nakano, Y. Minami, and S.-i. Sasa, Long-range phase order in two dimensions under shear flow, *Phys. Rev. Lett.* **126**, 160604 (2021).
- [8] S. F. Edwards and D. R. Wilkinson, The surface statistics of a granular aggregate, *Proc. R. Soc. Lond. A* **381**, 17-31 (1982).
- [9] See Supplemental Material at [URL will be inserted by publisher] for derivations and detailed explanations.
- [10] M. Kardar, G. Parisi, and Y. Zhang, Dynamic scaling of growing interfaces, *Phys. Rev. Lett.* **56**, 889 (1986).
- [11] R. Kubo, M. Toda, and N. Hashitsume, *Statistical Physics II: Nonequilibrium Statistical Mechanics*, (Springer-Verlag, Berlin, Germany, 1991)
- [12] D. N. Zubarev, *Nonequilibrium Statistical Thermodynamics*, (Consultants Bureau, New York, 1974)
- [13] J. A. McLennan, Statistical mechanics of transport in fluids, *Phys. Fluids* **3**, 493 (1960).
- [14] R. Landauer, Statistical physics of machinery: forgotten middle-ground, *Physica A* **194**, 551-562 (1993).
- [15] A. Dhar, Heat transport in low-dimensional systems, *advances in physics* **57**, 457-537 (2008).
- [16] D. Forster, D. R. Nelson, and M. J. Stephen, Large-distance and long-time properties of a randomly stirred fluid, *Phys. Rev. A* **16**, 732 (1977).
- [17] S. Lepri (Ed.), *Thermal Transport in Low Dimensions. From Statistical Physics to Nanoscale Heat Transfer*, (Springer International Publishing, Cham, Switzerland, 2016)
- [18] T. Halpin-Healy and K. A. Takeuchi, A KPZ Cocktail-shaken, not stirred: toasting 30 years of kinetically roughened surfaces, *J. Stat. Phys.* **160**, 794-814 (2015).
- [19] P. Meakin, The growth of rough surfaces and interfaces, *Physics Reports* **235**, 189-289 (1993).
- [20] T. J. Newman and A. J. Bray, Strong-coupling behaviour in discrete Kardar - Parisi - Zhang equations, *J. Phys. A: Math. Gen.* **29**, 7917-7928 (1996).
- [21] C. Lam and F. G. Shin, Anomaly in numerical integrations of the Kardar-Parisi-Zhang equation, *Phys. Rev. E* **57**, 6506-6511 (1998).
- [22] V. G. Miranda and F. D. A. A. Reis, Numerical study of the Kardar-Parisi-Zhang equation, *Phys. Rev. E* **77**, 031134 (2008)
- [23] H. S. Wio, J. A. Revelli, R. R. Deza, C. Escudero, and M. S. de La Lama, Discretization-related issues in the Kardar-Parisi-Zhang equation: Consistency, Galilean-invariance violation, and fluctuation-dissipation relation, *Phys. Rev. E* **81**, 066706 (2010)
- [24] M. Dentz, I. Neuweiler, Y. Méheust, and D. M. Tartakovsky, Noise-driven interfaces and their macroscopic representation, *Phys. Rev. E* **94**, 052802 (2016).
- [25] Priyanka, U. C. Täuber, and M. Pleimling, Feedback control of surface roughness in a one-dimensional Kardar-Parisi-Zhang growth process, *Phys. Rev. E* **101**, 022101 (2020).
- [26] H. van Beijeren, R. Kutner, and H. Spohn, Excess noise for driven diffusive systems, *Phys. Rev. Lett.* **54**, 2026-2029 (1985).
- [27] E. Medina, T. Hwa, M. Kardar, and Y. Zhang, Burgers equation with correlated noise: Renormalization-group analysis and applications to directed polymers and interface growth, *Phys. Rev. A* **39**, 3053-3075 (1989).
- [28] E. Frey and U. C. Täuber, Two-loop renormalization-group analysis of the Burgers-Kardar-Parisi-Zhang equation, *Phys. Rev. E* **50**, 1024-1045 (1994).
- [29] F. Colaiori and M. A. Moore, Numerical solution of the mode-coupling equations for the Kardar-Parisi-Zhang equation in one dimension, *Phys. Rev. E* **65**, 017105 (2001).
- [30] M. Prähofer and H. Spohn, Exact scaling functions for one-dimensional stationary KPZ growth, *J. Stat. Phys.* **115**, 255-279 (2004).
- [31] L. Canet, H. Chaté, B. Delamotte, and N. Wschebor, Nonperturbative renormalization group for the Kardar-Parisi-Zhang equation: General framework and first applications, *Phys. Rev. E* **84**, 061128 (2011).
- [32] O. Niggemann and U. Seifert, The two scaling regimes of the thermodynamic uncertainty relation for the KPZ equation, *J. Stat. Phys.* **186**, 1-29 (2022).
- [33] T. Sasamoto and H. Spohn, One-dimensional Kardar-Parisi-Zhang equation: An exact solution and its universality, *Phys. Rev. Lett.* **104**, 230602 (2010).
- [34] V. Dotsenko, Bethe ansatz derivation of the Tracy-Widom distribution for one-dimensional directed polymers, *Europhys. Lett.* **90**, 20003 (2010).
- [35] P. Calabrese, P. L. Doussal, and A. Rosso, Free-energy distribution of the directed polymer at high temperature,

- Europhys. Lett. **90**, 20002 (2010).
- [36] G. Amir, I. Corwin, and J. Quastel, Probability distribution of the free energy of the continuum directed random polymer in $1 + 1$ dimensions, *Communications on Pure and Applied Mathematics* **64**, 466-537 (2011).
- [37] T. Kloss, L. Canet, and N. Wschebor, Nonperturbative renormalization group for the stationary Kardar-Parisi-Zhang equation: Scaling functions and amplitude ratios in $1+1$, $2+1$, and $3+1$ dimensions, *Phys. Rev. E* **86**, 051124 (2012).
- [38] T. Imamura and T. Sasamoto, Stationary correlations for the 1D KPZ equation, *J. Stat. Phys.* **150**, 908-939 (2013).
- [39] M. Hairer, Solving the KPZ equation, *Annals of Mathematics* **178**, 559-664 (2013).
- [40] K. Johansson, The two-time distribution in geometric last-passage percolation, *Probab. Theory Relat. Fields* **175**, 849-895 (2019).
- [41] D. J. Evans, E. G. D. Cohen, and G. P. Morriss, Probability of second law violations in shearing steady states, *Phys. Rev. Lett.* **71**, 2401 (1993).
- [42] G. Gallavotti and E. G. D. Cohen, Dynamical ensembles in nonequilibrium statistical mechanics, *Phys. Rev. Lett.* **74**, 2694 (1995).
- [43] J. Kurchan, Fluctuation theorem for stochastic dynamics, *J. Phys. A: Math. Gen.* **31**, 3719 (1998).
- [44] U. Seifert, Stochastic thermodynamics, fluctuation theorems and molecular machines, *Rep. Prog. Phys.* **75**, 126001 (2012).
- [45] S.-i. Sasa, A fluctuation theorem for phase turbulence of chemical oscillatory waves, arXiv:nlin/0010026 (2000).
- [46] P. C. Martin, E. D. Siggia, and H. A. Rose, Statistical dynamics of classical systems, *Phys. Rev. A* **8**, 423-437 (1973).
- [47] H. Janssen, On a Lagrangean for classical field dynamics and renormalization group calculations of dynamical critical properties, *Z. Phys. B* **23**, 377-380 (1976).
- [48] U. Dekker and F. Haake, Fluctuation-dissipation theorems for classical processes, *Phys. Rev. A* **11**, 2043-2056 (1975).
- [49] K. A. Takeuchi, Experimental approaches to universal out-of-equilibrium scaling laws: turbulent liquid crystal and other developments, *J. Stat. Mech.* **2014**, P01006 (2014).
- [50] V. Yakhot, Large-scale properties of unstable systems governed by the Kuramoto-Sivashinski equation, *Phys. Rev. A* **24**, 642(R) (1981).
- [51] F. Hayot, C. Jayaprakash, and C. Josserand, Long-wavelength properties of the Kuramoto-Sivashinsky equation, *Phys. Rev. E* **47**, 911 (1993).
- [52] K. Ueno, H. Sakaguchi, and M. Okamura, Renormalization-group and numerical analysis of a noisy Kuramoto-Sivashinsky equation in $1 + 1$ dimensions, *Phys. Rev. E* **71**, 046138 (2005).
- [53] Y. Minami and S.-i. Sasa, The most effective model for describing the universal behavior of unstable surface growth, *J. Stat. Phys.* **173**, 120-139 (2018).

Supplemental Material: Divergent stiffness of a growing interface

Mutsumi Minoguchi and Shin-ichi Sasa

Throughout the supplemental material, we set $\nu = \kappa/\gamma$, $D = T/\gamma$, $\lambda = v_0$, and $\tilde{\epsilon} = \epsilon/\gamma$. The equation we study is then expressed as

$$\partial_t h = \nu \partial_x^2 h + \frac{\lambda}{2} (\partial_x h)^2 + \sqrt{2D} \xi + \tilde{\epsilon} p_{\text{ex}}(x), \quad (\text{S.1})$$

which is a forced KPZ equation with the most standard notation. The noise $\xi = \xi(x, t)$ satisfies

$$\langle \xi(x, t) \rangle = 0, \quad (\text{S.2})$$

$$\langle \xi(x, t) \xi(y, s) \rangle = \delta(x - y) \delta(t - s). \quad (\text{S.3})$$

We particularly focus on the case

$$p_{\text{ex}}(x) = \delta(x) - \frac{1}{L}, \quad (\text{S.4})$$

and the periodic boundary condition is assumed for $0 \leq x \leq L$.

The organization of the supplemental material is as follows. First, we summarize the basic issues of the equation we study. Then, in Sec. II, we derive the formulas presented in the main text. In Sec. III, we show some numerical results supporting arguments in the main text.

I. BASIC ISSUES

A. Dimensional analysis

A solution of (S.1) with a parameter set $(\nu, D, \lambda, L, \tilde{\epsilon})$ is connected to another solution of (S.1) with a different parameter set $(\nu', D', \lambda', L', \tilde{\epsilon}')$ by some scaling transformations. We explicitly confirm this fact, which is useful to derive a general expression of the effective surface tension.

First, we introduce coordinate transformations

$$x = \alpha_x x', \quad (\text{S.5a})$$

$$t = \alpha_t t', \quad (\text{S.5b})$$

where $\alpha_x > 0$ and $\alpha_t > 0$ are scaling factors. Accordingly, $0 \leq x' \leq L'$ with $L' = L/\alpha_x$. We also define $h'(x', t')$ by

$$h(x, t) = \alpha_h h'(x', t') \quad (\text{S.6})$$

with a new scaling factor $\alpha_h > 0$. Finally, we introduce $\xi'(x', t')$ that satisfies

$$\langle \xi'(x', t') \rangle = 0, \quad (\text{S.7})$$

$$\langle \xi'(x', t') \xi'(y', s') \rangle = \delta(x' - y') \delta(t' - s'). \quad (\text{S.8})$$

This is explicitly written as

$$\xi(x, t) = \alpha_x^{1/2} \alpha_t^{1/2} \xi'(x', t'). \quad (\text{S.9})$$

By substituting these relations into (S.1) with (S.4), we obtain

$$\partial_{t'} h' = \alpha_t \alpha_x^{-2} \nu \partial_{x'}^2 h' + \alpha_t \alpha_x^{-2} \alpha_h \frac{\lambda}{2} (\partial_{x'} h')^2 + \alpha_x^{-1/2} \alpha_t^{1/2} \alpha_h^{-1} \sqrt{2D} \xi' + \alpha_t \alpha_x^{-1} \alpha_h^{-1} \tilde{\epsilon} \left(\delta(x') - \frac{1}{L'} \right). \quad (\text{S.10})$$

From this expression, we define a new set of parameters $(\nu', D', \lambda', \tilde{\epsilon}')$ by

$$\alpha_t \alpha_x^{-2} \nu = \nu', \quad (\text{S.11a})$$

$$\alpha_t \alpha_x^{-2} \alpha_h \frac{\lambda}{2} = \frac{\lambda'}{2}, \quad (\text{S.11b})$$

$$\alpha_x^{-1/2} \alpha_t^{1/2} \alpha_h^{-1} \sqrt{2D} = \sqrt{2D'}, \quad (\text{S.11c})$$

$$\alpha_t \alpha_x^{-1} \alpha_h^{-1} \tilde{\epsilon} = \tilde{\epsilon}', \quad (\text{S.11d})$$

so that (S.10) becomes

$$\partial_{t'} h' = \nu' \partial_{x'}^2 h' + \frac{\lambda'}{2} (\partial_{x'} h')^2 + \sqrt{2D'} \xi' + \tilde{\epsilon}' \left(\delta(x') - \frac{1}{L'} \right). \quad (\text{S.12})$$

By solving (S.11), we find

$$\alpha_x = \frac{r_\nu^3}{r_D r_\lambda^2}, \quad (\text{S.13a})$$

$$\alpha_t = \frac{r_\nu^5}{r_D^2 r_\lambda^4}, \quad (\text{S.13b})$$

$$\alpha_h = \frac{r_\nu}{r_\lambda}, \quad (\text{S.13c})$$

$$r_{\tilde{\epsilon}} = \frac{r_\lambda r_D}{r_\nu}, \quad (\text{S.13d})$$

where $r_\nu = \nu/\nu'$, $r_\lambda = \lambda/\lambda'$, $r_D = D/D'$, and $r_{\tilde{\epsilon}} = \tilde{\epsilon}/\tilde{\epsilon}'$. That is, by appropriately choosing α_x , α_t , and α_h for (S.1), we obtain a different model with ν' , D' , and λ' whose values are specified.

B. Discrete model

In numerical simulations of (S.1), we define a discrete field $h_i(t) \equiv h(i\Delta x, t)$ with $0 \leq i \leq N$, where Δx is a numerical parameter, $N\Delta x = L$, and $h_0 = h_N$. Throughout this study, we fix $\Delta x = 0.5$. For later convenience, we also define

$$u_i(t) \equiv \frac{h_{i+1}(t) - h_i(t)}{\Delta x}, \quad (\text{S.14})$$

which represents a discrete field corresponding to $u(x, t) = \partial_x h(x, t)$. We then study the following discrete model of (S.1):

$$\frac{dh_i}{dt} = \nu \frac{u_i - u_{i-1}}{\Delta x} + \frac{\lambda}{6} (u_i^2 + u_i u_{i-1} + u_{i-1}^2) + \tilde{\epsilon} p_{\text{ex}i} + \sqrt{\frac{2D}{\Delta x}} \xi_i, \quad (\text{S.15})$$

where $\xi_i(t)$ is Gaussian white noise that satisfies $\langle \xi_i(t) \rangle = 0$ and $\langle \xi_i(t) \xi_j(t') \rangle = \delta_{ij} \delta(t - t')$. $\tilde{\epsilon} p_{\text{ex}i}$ is a discrete form of the external stress $\epsilon p_{\text{ex}}(x)$. It can be seen that (S.15) leads to (S.1) in the limit $\Delta x \rightarrow 0$.

We express (u_0, \dots, u_{N-1}) as \mathbf{u} collectively. The stationary distribution of \mathbf{u} for $\epsilon = 0$ is then calculated as

$$P_0^{\text{ss}}(\mathbf{u}) = \left(\frac{\nu(\Delta x)}{2D\pi} \right)^{N/2} \exp \left[-\frac{\nu}{2D} \sum_i (\Delta x) u_i^2 \right]. \quad (\text{S.16})$$

More precisely, the non-linear term in (S.15) is chosen so that (S.16) holds [21]. See (S.28) for the argument. We used the Heun method to solve (S.15) numerically, and we confirmed that the numerical estimation of $\langle u_i^2 \rangle$ is equal to the theoretical value within 1% error for $\Delta t = 0.01$.

Here, we note that (S.15) is rewritten as the continuity equation

$$\frac{du_i}{dt} + \frac{j_{i+1} - j_i}{\Delta x} = 0, \quad (\text{S.17})$$

where the current field is given as

$$j_i \equiv -\frac{\lambda}{6} (u_i^2 + u_i u_{i-1} + u_{i-1}^2) - \nu \frac{u_i - u_{i-1}}{\Delta x} - \tilde{\epsilon} p_{\text{ex}i} - \sqrt{\frac{2D}{\Delta x}} \xi_i. \quad (\text{S.18})$$

The trajectory $(\mathbf{u}(t))_{t=0}^\tau$ is collectively denoted by $[\mathbf{u}]$. Let $\mathcal{P}([\mathbf{u}]|\mathbf{u}(0))$ be the probability density of trajectory $[\mathbf{u}]$ provided that $\mathbf{u}(0)$ is given. From the Gaussian nature of ξ_i , we first have

$$\mathcal{P}([\mathbf{u}]|\mathbf{u}(0)) = \mathcal{N} \exp \left[-\frac{\Delta x}{4D} \int_0^\tau dt \sum_{i=1}^N \left(\frac{\lambda}{6} (u_i^2 + u_i u_{i-1} + u_{i-1}^2) + \nu \frac{u_i - u_{i-1}}{\Delta x} + \tilde{\epsilon} p_{\text{ex}i} + j_i \right)^2 \right], \quad (\text{S.19})$$

where the periodic boundary conditions have been used in the derivation. The time integration is evaluated as the mid-point discretization and \mathcal{N} is the normalization constant which depends on the time interval Δt in the time integration.

C. Time-reversal symmetry

We define two types of time-reversal transformation, $u_i^*(t) \equiv u_i(\tau - t)$ and $u_i^\dagger(t) \equiv -u_i(\tau - t)$. Associated with them, we have the following two relations respectively. The first relation is

$$\frac{\mathcal{P}([\mathbf{u}^*]|\mathbf{u}^*(0))}{\mathcal{P}([\mathbf{u}]|\mathbf{u}(0))} = \exp(-\sigma[\mathbf{u}]) \exp(\beta F^\epsilon(\mathbf{h}(\tau)) - \beta F^\epsilon(\mathbf{h}(0))) \quad (\text{S.20})$$

with

$$\sigma([\mathbf{u}]) \equiv \frac{1}{D} \int_0^\tau dt \sum_i (\Delta x) \frac{dh_i}{dt} \frac{\lambda}{6} (u_i^2 + u_i u_{i-1} + u_{i-1}^2) \quad (\text{S.21})$$

and

$$F^\epsilon(\mathbf{h}) = \gamma \sum_i (\Delta x) \left[\frac{\nu}{2} u_i^2 - \tilde{\epsilon} p_{\text{ex}i} h_i \right]. \quad (\text{S.22})$$

Here, in the calculation of (S.20), we have used

$$\frac{dF^\epsilon(\mathbf{h}(t))}{dt} = \sum_i \frac{dh_i}{dt} \frac{\partial F^\epsilon(\mathbf{h})}{\partial h_i}. \quad (\text{S.23})$$

When $\lambda = 0$, (S.20) implies the detailed balance condition with respect to the equilibrium distribution proportional to $\exp[-\beta F^\epsilon(\mathbf{h})]$.

The second one is

$$\frac{\mathcal{P}([\mathbf{u}^\dagger]|\mathbf{u}^\dagger(0))}{\mathcal{P}([\mathbf{u}]|\mathbf{u}(0))} = \exp(-\tilde{\sigma}([\mathbf{u}])) \exp \left(\frac{\nu}{2D} \sum_i u_i^2(\tau) \Delta x - \frac{\nu}{2D} \sum_i u_i^2(0) \Delta x \right) \quad (\text{S.24})$$

with

$$\tilde{\sigma}([\mathbf{u}]) \equiv -\frac{\nu}{D} \int_0^\tau dt \sum_i \tilde{\epsilon} p_{\text{ex}i} (u_i - u_{i-1}). \quad (\text{S.25})$$

In the derivation of (S.24), we have used

$$\sum_i \partial_t (u_i^2) = -\frac{2}{\Delta x} \sum_i (u_i j_{i+1} - u_i j_i) \quad (\text{S.26})$$

$$= \frac{2}{\Delta x} \sum_i (u_i - u_{i-1}) j_i, \quad (\text{S.27})$$

and

$$\sum_i (u_i^2 + u_i u_{i-1} + u_{i-1}^2) (u_i - u_{i-1}) = 0. \quad (\text{S.28})$$

When $\epsilon = 0$, (S.24) implies the detailed balance condition with respect to the distribution proportional to $\exp[-\nu/(2D) \sum_i u_i^2 \Delta x]$. This provides the proof of (S.16). Note that $\nu/(2D) \sum_i u_i^2 \Delta x$ is equal to $\beta F^0(\mathbf{h})$.

II. DERIVATION OF FORMULAS

A. Derivation of (5)

For equilibrium cases, the expectation of $h(x)$ under the external stress is determined by

$$\nu \frac{\partial^2}{\partial x^2} \langle h \rangle_{\text{eq}}^\epsilon + \tilde{\epsilon} \left(\delta(x) - \frac{1}{L} \right) = 0. \quad (\text{S.29})$$

Since $\partial_x^2 \langle h(x) \rangle_{\text{eq}}^\epsilon = 0$ for $x \neq 0$ and $\langle h(x) \rangle_{\text{eq}}^\epsilon = \langle h(L-x) \rangle_{\text{eq}}^\epsilon$, we have

$$\langle h(x) - h(0) \rangle_{\text{eq}}^\epsilon = C \left[\left(x - \frac{L}{2} \right)^2 - \frac{L^2}{4} \right], \quad (\text{S.30})$$

where C is a constant whose value is not determined yet. Furthermore, integrating (S.29) in the region $[0, \delta]$ and $[L - \delta, L]$ and taking the limit $\delta \rightarrow 0+$, we obtain

$$\nu \frac{\partial}{\partial x} \langle h \rangle_{\text{eq}}^\epsilon \Big|_{0+} - \nu \frac{\partial}{\partial x} \langle h \rangle_{\text{eq}}^\epsilon \Big|_{L-} + \tilde{\epsilon} = 0, \quad (\text{S.31})$$

where we have used the periodic boundary condition. This leads to $C = \tilde{\epsilon}/(2L\nu)$. Thus,

$$\langle h(x) - h(0) \rangle_{\text{eq}}^\epsilon = \frac{\tilde{\epsilon}}{2L\nu} \left[\left(x - \frac{L}{2} \right)^2 - \frac{L^2}{4} \right]. \quad (\text{S.32})$$

By setting $x = L/2$, we also have

$$\langle h(L/2) - h(0) \rangle_{\text{eq}}^\epsilon = -\frac{L\tilde{\epsilon}}{8\nu}. \quad (\text{S.33})$$

B. Derivation of (10) and (11)

In this section, we study the discrete model defined in Sec. IB. We first note that \mathbf{h} is not uniquely determined from \mathbf{u} , because an additive constant of \mathbf{h} is arbitrary for given \mathbf{u} . Nevertheless, if a quantity $A(\mathbf{h})$ satisfies $A(\mathbf{h} + c\mathbf{1}) = A(\mathbf{h})$ for any c , where $\mathbf{1} = (1, 1, \dots, 1)$, we can uniquely express A in terms of \mathbf{u} . We thus write $A([\mathbf{u}])$, which we study in this section.

We first define

$$\langle A \rangle_I^{\text{tr}} \equiv \int \mathcal{D}[\mathbf{u}] A([\mathbf{u}]) \mathcal{P}(\mathbf{u}|\mathbf{u}(0)) P_{\text{eq}}^\epsilon(\mathbf{u}(0)), \quad (\text{S.34})$$

which represents the ensemble average of A over noise realizations and initial conditions sampled from the equilibrium distribution with $\lambda = 0$. Using (S.20), we obtain

$$\langle A \rangle_I^{\text{tr}} = \int \mathcal{D}[\mathbf{u}] A([\mathbf{u}^*]) \frac{\mathcal{P}([\mathbf{u}^*]|\mathbf{u}^*(0))}{\mathcal{P}([\mathbf{u}]|\mathbf{u}(0))} \mathcal{P}([\mathbf{u}]|\mathbf{u}(0)) P_{\text{eq}}^\epsilon(\mathbf{u}(t = \tau)) \quad (\text{S.35})$$

$$= \int \mathcal{D}[\mathbf{u}] A([\mathbf{u}^*]) \exp(-\sigma([\mathbf{u}])) \mathcal{P}([\mathbf{u}]|\mathbf{u}(0)) P_{\text{eq}}^\epsilon(\mathbf{u}(t = 0)) \quad (\text{S.36})$$

$$= \langle A^* e^{-\sigma} \rangle_I^{\text{tr}}, \quad (\text{S.37})$$

where $A^*([\mathbf{u}]) \equiv A([\mathbf{u}^*])$. This is the standard form of the fluctuation theorem, and σ corresponds to the thermodynamic entropy production in the system we study.

Since we have the second relation (S.24) associated with time-reversal transformation, we further define

$$\langle A \rangle_{II}^{\text{tr}} \equiv \int \mathcal{D}[\mathbf{u}] A([\mathbf{u}]) \mathcal{P}(\mathbf{u}|\mathbf{u}(0)) P_{\text{ss}}^0(\mathbf{u}(0)), \quad (\text{S.38})$$

which represents the ensemble average of A over noise realizations and initial conditions sampled from the stationary distribution with $\epsilon = 0$. Using (S.24), we obtain

$$\langle A \rangle_{II}^{\text{tr}} = \int \mathcal{D}[\mathbf{u}] A([\mathbf{u}^\dagger]) \frac{\mathcal{P}([\mathbf{u}^\dagger]|\mathbf{u}^\dagger(0))}{\mathcal{P}([\mathbf{u}|\mathbf{u}(0))} \mathcal{P}([\mathbf{u}|\mathbf{u}(0)) P_{\text{ss}}^0(\mathbf{u}(t=\tau)) \quad (\text{S.39})$$

$$= \int \mathcal{D}[\mathbf{u}] A([\mathbf{u}^\dagger]) \exp(-\tilde{\sigma}([\mathbf{u}])) \mathcal{P}([\mathbf{u}|\mathbf{u}(0)) P_{\text{ss}}^0(\mathbf{u}(t=0)) \quad (\text{S.40})$$

$$= \langle A^\dagger e^{-\tilde{\sigma}} \rangle_{II}^{\text{tr}}, \quad (\text{S.41})$$

where $A^\dagger([\mathbf{u}]) \equiv A([\mathbf{u}^\dagger])$. This fluctuation theorem is not standard, since $\tilde{\sigma}$ does not correspond to the thermodynamic entropy. Instead, $\tilde{\sigma}$ is interpreted as the excess entropy production that characterizes the extent of the violation of time-reversal symmetry in the KPZ equation.

C. Derivation of (13)

Setting $A = u_i(\tau)$ and substituting $p_{\text{ex}i} = \delta_{i0}/\Delta x - 1/L$ into (S.41), we have

$$\langle u_i(\tau) \rangle_{II}^{\text{tr}} = \left\langle -u_i(0) e^{\frac{\nu\tilde{\epsilon}}{D\Delta x} \int_0^\tau dt (u_{0,t} - u_{N-1,t})} \right\rangle_{II}^{\text{tr}}. \quad (\text{S.42})$$

Then we expand it in $\tilde{\epsilon}$ and take the limit $\tau \rightarrow \infty$. Noting that

$$\lim_{\tau \rightarrow \infty} \langle u_i(\tau) \rangle_{II}^{\text{tr}} = \langle u_i \rangle_{\text{ss}}^\epsilon, \quad (\text{S.43})$$

we obtain

$$\langle u_i \rangle_{\text{ss}}^\epsilon = -\frac{\nu\tilde{\epsilon}}{D\Delta x} \int_0^\infty dt \langle u_i(0)(u_0(t) - u_{N-1}(t)) \rangle_{\text{ss}}^0 + \mathcal{O}(\epsilon^2) \quad (\text{S.44})$$

$$= \frac{\nu\tilde{\epsilon}}{D\Delta x} \int_0^\infty dt \left(\langle u_{i+1}(0)u_0(t) \rangle_{\text{ss}}^0 - \langle u_i(0)u_0(t) \rangle_{\text{ss}}^0 \right) + \mathcal{O}(\epsilon^2). \quad (\text{S.45})$$

Therefore, the response formula is derived as

$$\langle h_i - h_0 \rangle_{\text{ss}}^\epsilon = \sum_{j=0}^{i-1} \Delta x \langle u_j \rangle_{\text{ss}}^\epsilon \quad (\text{S.46})$$

$$= \sum_{j=0}^{i-1} \frac{\nu\tilde{\epsilon}}{D} \int_0^\infty dt \left(\langle u_{j+1}(0)u_0(t) \rangle_{\text{ss}}^0 - \langle u_j(0)u_0(t) \rangle_{\text{ss}}^0 \right) + \mathcal{O}(\epsilon^2) \quad (\text{S.47})$$

$$= \frac{\nu\tilde{\epsilon}}{D} \int_0^\infty dt \left(\langle u_i(0)u_0(t) \rangle_{\text{ss}}^0 - \langle u_0(0)u_0(t) \rangle_{\text{ss}}^0 \right) + \mathcal{O}(\epsilon^2) \quad (\text{S.48})$$

$$= \frac{\nu\tilde{\epsilon}}{D} \int_0^\infty dt (C_i(t) - C_0(t)) + \mathcal{O}(\epsilon^2), \quad (\text{S.49})$$

where $C_i(t) \equiv \langle u_i(0)u_0(t) \rangle_{\text{ss}}^0$. Taking the limit $\Delta x \rightarrow 0$, we have

$$\langle h(x) - h(0) \rangle_{\text{ss}}^\epsilon = \frac{\nu\tilde{\epsilon}}{D} \int_0^\infty dt (C(x,t) - C(0,t)) + \mathcal{O}(\epsilon^2) \quad (\text{S.50})$$

with $C(x,t) \equiv \langle u(x,0)u(0,t) \rangle_{\text{ss}}^0$.

D. Derivation of (17)

We consider ν_{eff}/ν for the model (S.1). We choose α_x , α_t , and α_h such that $\nu' = D' = \lambda' = 1$. We then have ν'_{eff} is given as a function of L' , which is simply written as

$$\nu'_{\text{eff}} = f\left(\frac{L'}{\ell}\right), \quad (\text{S.51})$$

where ℓ is a numerical constant characterizing the dimensionless crossover length. Since $\nu_{\text{eff}}/\nu = \nu'_{\text{eff}}$, we obtain

$$\frac{\nu_{\text{eff}}}{\nu} = f\left(\frac{L}{\ell\alpha_x}\right) = f\left(\frac{D\lambda^2 L}{\ell\nu^3}\right). \quad (\text{S.52})$$

Thus, setting

$$L_0 = \ell \frac{\nu^3}{D\lambda^2}, \quad (\text{S.53})$$

we obtain the formula (17) in the main text.

E. Estimation of c in (20)

We define the space-time Fourier transform of $C(x, t)$ as

$$\check{C}(k, \omega) \equiv \int_{-\infty}^{\infty} dx \int_{-\infty}^{\infty} dt e^{i(kx + \omega t)} C(x, t). \quad (\text{S.54})$$

We then have

$$\int_0^{\infty} dt \check{C}(k, t) = \frac{1}{2} \check{C}(k, 0), \quad (\text{S.55})$$

because $\check{C}(k, t) = \check{C}(k, -t)$. Here, Prähofer and Spohn showed that

$$\check{C}(k, 0) = 9.72216k^{-3/2} \quad (\text{S.56})$$

for an exactly solvable stochastic model that corresponds to the KPZ equation with $D/\nu = 1$ and $\lambda = 1/2$ [S1]. From (19) and (20) in the main text, we write

$$\int_0^{\infty} dt \check{C}(k, t) = c \left(\frac{D}{\nu\lambda^2}\right)^{1/2} k^{-3/2}, \quad (\text{S.57})$$

which becomes

$$\int_0^{\infty} dt \check{C}(k, t) = 2ck^{-3/2} \quad (\text{S.58})$$

for the system with $D/\nu = 1$ and $\lambda = 1/2$. Comparing this expression and (S.55) with (S.56), we obtain $c = 2.43054$.

F. Derivation of (21)

We first consider the Fourier expansion

$$\int_0^{\infty} dt C(x, t) = \frac{1}{L} \sum_{n=-n_c}^{n_c} C_n e^{-ik_n x} \quad (\text{S.59})$$

with $k_n = 2\pi n/L$, where the cut-off number n_c is given by $L/(2\Delta x)$. From (S.57), we may set

$$C_n = c \left(\frac{D}{\nu\lambda^2}\right)^{1/2} k_n^{-3/2} \quad (\text{S.60})$$

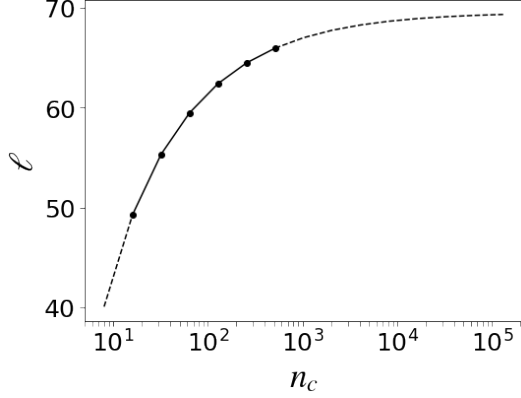


FIG. S.1. n_c dependence of ℓ expressed by (S.64). The solid line shows the range of values we used in our numerical calculations.

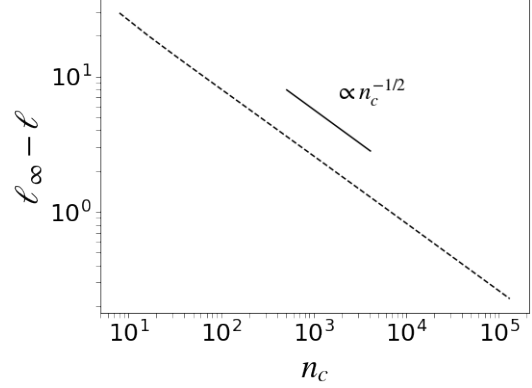


FIG. S.2. Asymptotic behavior of ℓ converging to ℓ_∞ given in (S.65). The relation $\ell_\infty - \ell = 80n_c^{-1/2}$ holds for large n_c .

for sufficiently large L . We then find

$$\begin{aligned}
 & \int_0^\infty dt \left[C\left(\frac{L}{2}, t\right) - C(0, t) \right] \\
 &= \frac{c}{L} \left(\frac{D}{\nu\lambda^2} \right)^{1/2} \sum_{n=-n_c}^{n_c} ((-1)^n - 1) \frac{1}{k_n^{3/2}} \\
 &= -\frac{4c}{L} \left(\frac{L}{2\pi} \right)^{3/2} \left(\frac{D}{\nu\lambda^2} \right)^{1/2} \sum_{n=1}^{n_c/2} \frac{1}{(2n-1)^{3/2}}. \tag{S.61}
 \end{aligned}$$

Substituting this result into the formula (15) in the main text, we obtain the form

$$\kappa_{\text{eff}} = \kappa \left(\frac{L}{L_0} \right)^{1/2}, \tag{S.62}$$

where L_0 is calculated as

$$L_0 = \ell \frac{\nu^3}{D\lambda^2} \tag{S.63}$$

with

$$\ell = \frac{(32c)^2}{(2\pi)^3} \left(\sum_{n=1}^{n_c/2} \frac{1}{(2n-1)^{3/2}} \right)^2. \tag{S.64}$$

This gives the estimation of the dimensionless cross-over length ℓ defined by (16) and (18) in the main text.

In Fig. S.1, we plot ℓ for n_c . In the range we studied in numerical simulations, the theoretical estimation of ℓ is consistent with the numerically obtained value $\ell \simeq 60$. If we study the case that $L \rightarrow \infty$, ℓ should be evaluated in the limit $n_c \rightarrow \infty$. This value, which is denoted by ℓ_∞ , is calculated as

$$\begin{aligned}
 \ell_\infty &= \frac{(32c)^2}{(2\pi)^3} \left(\sum_{n=1}^{\infty} \frac{1}{n^{3/2}} - \sum_{n=1}^{\infty} \frac{1}{(2n)^{3/2}} \right)^2 \\
 &= \frac{(32c)^2}{(2\pi)^3} \left(1 - \frac{1}{2^{3/2}} \right)^2 \zeta\left(\frac{3}{2}\right)^2 \\
 &\simeq 69.52. \tag{S.65}
 \end{aligned}$$

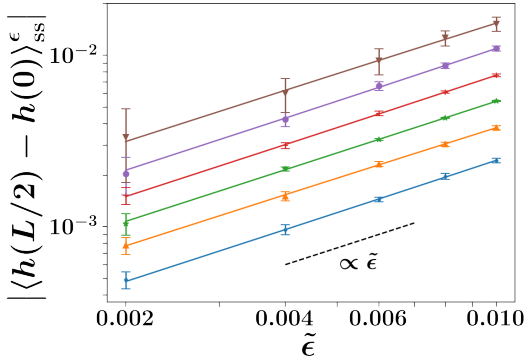


FIG. S.3. Amplitude of the averaged height function against the strength of the external stress for system sizes $L = 2, 4, 8, 16, 32,$ and 64 , from bottom to top. $v_0 = 5$. The symbols show the numerical results and they are fitted to a quadratic function $f_2 = c_1\tilde{\epsilon} + c_2\tilde{\epsilon}^2$ (solid lines).

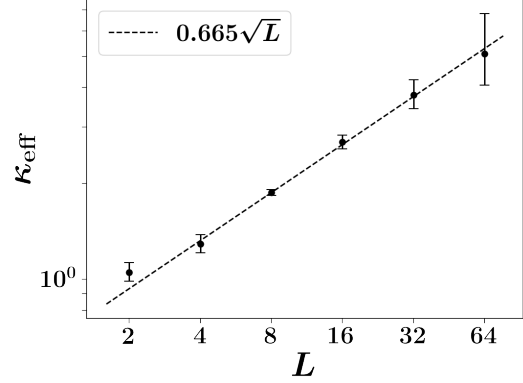


FIG. S.4. κ_{eff} calculated by (S.67) are displayed as a function of L . $v_0 = 5$. This shows the divergent behavior $\kappa_{\text{eff}} = 0.665\sqrt{L}$.

Note that the convergence is slow and Fig. S.2 shows that

$$\ell_\infty - \ell(n_c) = \frac{A}{\sqrt{n_c}} \quad (\text{S.66})$$

for large n_c , where $A = 80$.

III. SUPPLEMENTAL DATA

A. Measurement of the response

In Fig. 3 of the main text, we display the numerical data of $\langle h(L/2) - h(0) \rangle_{\text{ss}}^\epsilon / \tilde{\epsilon}$. Here, we explain the method for numerically evaluating it. In Fig. S.3, we show $\langle h(0) - h(L/2) \rangle_{\text{ss}}^\epsilon$ for several values of $\tilde{\epsilon}$ ranged from 0.002 to 0.01 for systems with sizes $L = 2, 4, 8, 16, 32,$ and 64 . For each L , we fit the data points by a quadratic function $f_2(\tilde{\epsilon}) = c_1\tilde{\epsilon} + c_2\tilde{\epsilon}^2$ by the least-square method. This linear coefficient c_1 is given as $\langle h(L/2) - h(0) \rangle_{\text{ss}}^\epsilon / \tilde{\epsilon}$ in Fig. 3 of the main text.

Using the coefficient c_1 and (7) in the main text, we have

$$\kappa_{\text{eff}} = \frac{L}{8c_1}. \quad (\text{S.67})$$

Then, we display κ_{eff} as a function of L in Fig. S.4. This graph already shows the \sqrt{L} behavior of κ_{eff} . However, it is hard to study larger systems than $L = 64$ by this method.

B. Dynamical-scaling exponent

It has been known that the dynamical exponent z is equal to $3/2$ for the KPZ equation. We directly confirm this fact by numerical simulations. Concretely, we study the height width

$$W(L, t) \equiv \sqrt{\langle (h - \langle h \rangle)^2 \rangle} \quad (\text{S.68})$$

for the initial condition $h(x, 0) = 0$. In Fig. S.5, we plot $W/L^{1/2}$ against $t/L^{3/2}$ for system sizes $L = 64, 256, 1024,$ and 4096 with $\nu = D = 1$ and $\lambda = 5$ fixed. It is found that all the data are on the same universal curve. The scaling function observed in the simulation is consistent with known results.

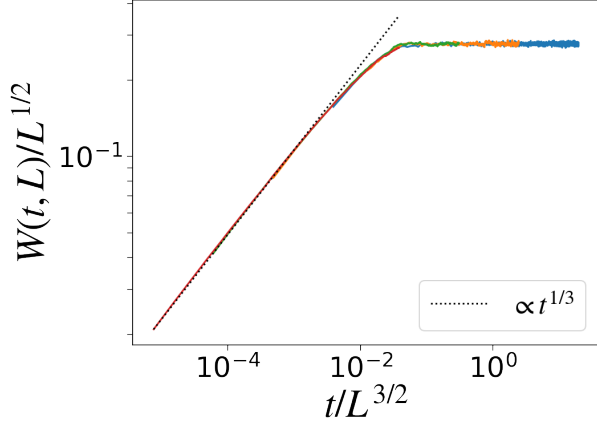


FIG. S.5. Dynamical scaling of the width W for the KPZ interface with $\lambda = 5$. The system sizes are $L = 64, 256, 1024$, and 4096 from right to left. The dotted line is a guide to the eye.

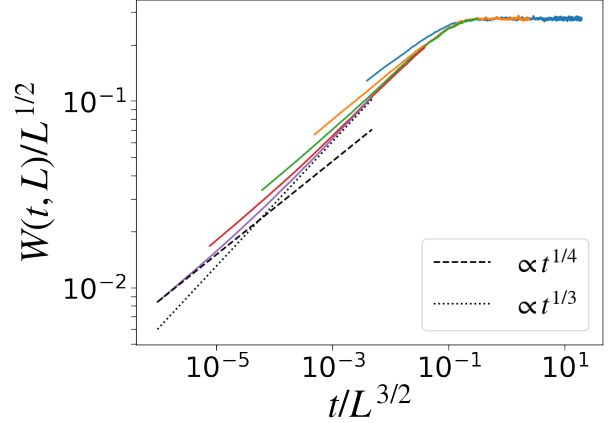


FIG. S.6. The same as Fig. S.5, but for $\lambda = 1$. The system sizes are $L = 64, 256, 1024, 4096$, and 16384 from right to left. In this case, the width grows as $t^{1/4}$ (dashed line), not $t^{1/3}$ (dotted line), until non-linearity grows enough.

We note that the same procedure does not yield a clear curve for the numerical simulations of the system with $\lambda = 1$, as shown in Fig. S.6. This is interpreted as a finite time effect. Concretely, in the early stage $t \ll t_0$, the growth of W is described by the linear (equilibrium) dynamics with $\lambda = 0$, while the non-linear growth effect becomes dominant for the late stage $t \gg t_0$. The cross-over time t_0 was numerically obtained [S2, S3, S4] as

$$t_0 \simeq 252\nu^5 D^{-2} \lambda^{-4}. \quad (\text{S.69})$$

We conjecture that the cross-over time t_0 is related to the cross-over length L_0 in our study.

C. Finite mesh effect for $\kappa_{\text{eff}}(L)$

Since we fix $\Delta x = 0.5$ in the discrete model, the model with small L may not provide a good approximation of the KPZ equation. In order to study this aspect more quantitatively, in Fig. S.7, we plot κ_{eff} against $L \geq 2$ with $v_0 = 5$ fixed. It shows that κ_{eff} is almost proportional to \sqrt{L} for $L \geq 4$. However, when we plot κ_{eff} for several values of v_0 in Fig. S.8, we find that the data for $L = 2, 4$, and 8 are not on the one universal curve. This means that the discrete model with $\Delta x = 0.5$ is not a good approximation of the KPZ equation with $L = 2, 4$, and 8 . More quantitatively, we notice that the cut-off number $n_c = L/(2\Delta x)$ characterizes the cross-over length as shown in (S.64) and Fig. S.1. This means that the system with smaller n_c shows a shorter cross-over length, which makes the data points shift to the right side. Therefore, the data for the systems with small L are obviously contaminated by discretization effects and thus deviate from the universal curve determined in the larger systems. For this reason, we employ the data for $L \geq 16$ in the main text.

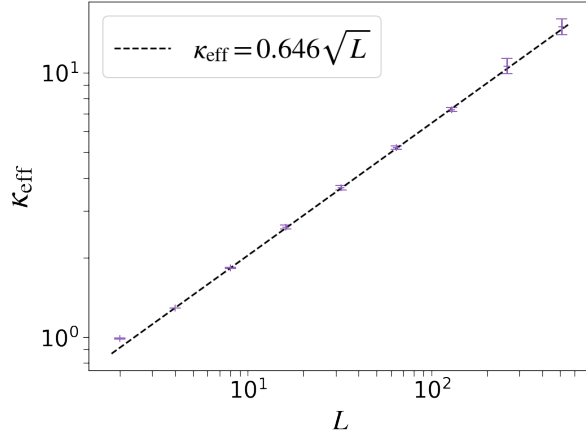


FIG. S.7. κ_{eff} for $L = 2, 4, 8, 16, 32, 64, 128, 256,$ and 512 from left to right. $v_0 = 5$. The symbols $L \geq 4$ are on the straight line corresponding to $\kappa_{\text{eff}} = 0.646\sqrt{L}$.

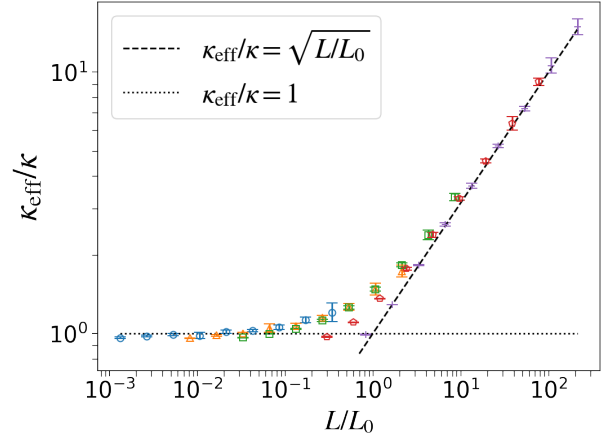


FIG. S.8. κ_{eff} for the same system sizes as Fig. S.7 and with $v_0 = 0.2, 0.5, 1, 3,$ and 5 (difference in symbols represents the difference in v_0). L_0 is given by (S.63) with $\ell \simeq 60$ in this figure. The symbols for the small system sizes $L = 2, 4,$ and 8 are not in the universal curve.

[S1] See (5.9) and (5.11) in Ref. [30].

[S2] J. Krug, Origins of scale invariance in growth processes, *Advances in Physics* **46**, 139-282 (1996).

[S3] T. Halpin-Healy and Y. Zhang, Kinetic roughening phenomena, stochastic growth, directed polymers and all that. *Aspects of multidisciplinary statistical mechanics*, *Physics Reports* **254**, 215-414 (1995).

[S4] K. Sneppen, J. Krug, M. H. Jensen, C. Jayaprakash and T. Bohr, Dynamic scaling and crossover analysis for the Kuramoto-Sivashinsky equation, *Phys. Rev. A* **46**, R7351(R) (1992).